LARGE-SCALE ROTATIONAL MOTIONS OF PROTEINS DETECTED BY ELECTRON PARAMAGNETIC RESONANCE AND FLUORESCENCE

DAVID D. THOMAS, *Department of Structural Biology, Sherman Fairchild Center, Stanford University School of Medicine, Stanford, California 94305 U. S. A.*

ABSTRACT Direct spectroscopic measurements of rotational motions of proteins and large protein segments are crucial to understanding the molecular dynamics of protein function. Fluorescent probes and spin labels attached to proteins have proved to be powerful tools in the study of large-scale protein motions. Fluorescence depolarization and conventional electron paramagnetic resonance (EPR) are applicable to the study of rotational motions in the nanosecond-to-microsecond time range, and have been used to demonstrate segmental flexibility in an antibody and in myosin. Very slow rotational motions, occurring in the microsecond-to-millisecond time range, are particularly important in supramolecular assemblies, where protein motions are restricted by association with other molecules. Saturation transfer spectroscopy (ST-EPR), a recently developed electron paramagnetic resonance (EPR) technique that permits the detection of rotational correlation times as long as 1 ms, has been used to detect large-scale rotational motions of spin-labeled proteins in muscle filaments and in membranes, providing valuable insights into energy transduction mechanisms in these assemblies.

INTRODUCTION

In recent years there has been a rapid accumulation of biochemical and structural information about large proteins and organized supramolecular assemblies containing proteins, such as membranes, contractile filaments, chromosomes, and ribosomes. A central goal of biophysicists is to describe the roles of these proteins in precise physical terms. In most of the interesting cases, these roles are dynamic, involving biochemical reactions and energy transduction, so this goal can be achieved only by combining biochemical and structural information with direct measurements of molecular motions. Large-scale motions, i.e., motions of whole proteins or large segments of proteins, are particularly important. These motions are likely to affect the direct interaction of a protein with other macromolecules, and are likely to be important links between microscopic and macroscopic dynamics, in processes involving energy transduction. For example, the ATP-driven motions of large segments of muscle proteins are thought to be transduced directly into motions of whole assemblies (filaments) of these proteins and eventually into contraction of the muscle (1–3). The motions of

BIOPHYS. J. © Biophysical Society · 0006-3495/78/1101-439 $1.00
Volume 24 November 1978 439-462

membrane-bound enzymes, antibodies, and antigens relative to each other and to the surrounding lipids are postulated to be crucial to membrane function (4, 5).

Attached Probes: Advantages and Problems

The two methods discussed in detail in this review involve the use of motion-sensitive spectroscopic probe molecules, either fluorescent dyes or nitroxide spin labels, covalently (or at least very tightly) bound to proteins. The chief advantage of the use of probes like these is the opportunity to study selected components of complex systems. Without extrinsic probes, the investigator is usually limited to the study of a solution of an isolated, purified protein, using a technique sensitive to protein motions in general (e.g., light scattering, dielectric relaxation, or birefringence). The rotational motion detected by such nonselective methods is not easily ascribed to a particular region of a protein and is usually used to estimate the overall size and shape of a protein in solution, by assuming that it is a particular type of rigid body. This review is concerned primarily with motions likely to have clearly defined functional importance, such as the motion of a specific part of a protein or the motion of a specific protein in a complex functioning assembly. The selective detection of such motions often requires the use of motion-sensitive probes chemically directed at selected sites.

The experimental requirements for the use of probes in observing large-scale protein motions are much the same as in other applications of attached probes (6, 7). The spectrum of the probe must be sensitive to the phenomenon studied (in this case, slow rotational motion). The probe should be selectively reactive with the protein to be studied, and labeling should not seriously perturb the function of the protein. After labeling, it is important to verify, with other biochemical and physical measurements, that the protein's structure and function are essentially preserved. There remains the possibility that the motion is perturbed by labeling, despite the lack of any detectable change in protein function. However, in the study of large-scale protein motion this perturbation problem is likely to be less severe than in other applications, because the probe molecule is much smaller than the moiety whose motion is being probed. Unless the probe reacts directly with a crucial group on the protein, the probability is high that the large-scale motions are not significantly perturbed. To detect these motions, however, the probe must be rigidly attached to the protein, so that the motion of the probe is determined by the motion of the protein. This is a particularly important problem for the study of slow motion, and is the chief factor limiting the general applicability of the method. As shown below, however, the requirement of rigid binding has been met in a number of cases, making possible the direct measurement of important large-scale protein motions.

Techniques and Time Ranges

Large-scale rotational motions are likely to be slow on the molecular time scale. Motions of individual amino acid residues often occur in the picosecond-to-nanosecond time range, and we expect motions of large protein segments or whole proteins in

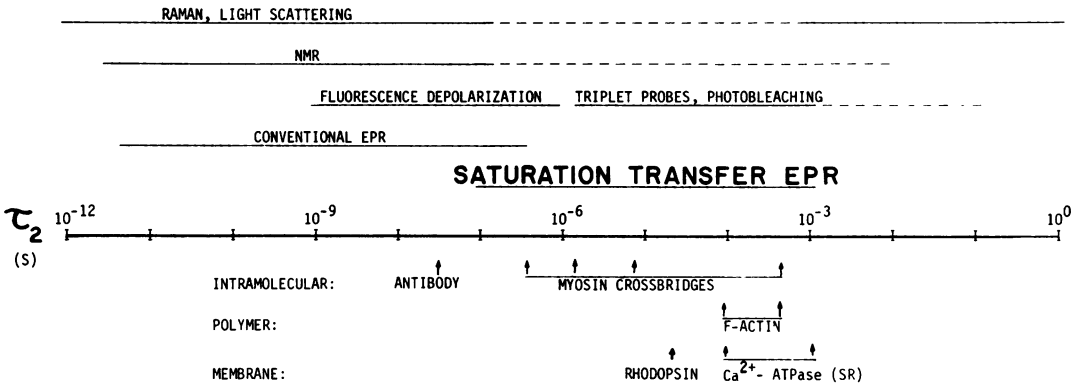

FIGURE 1 Techniques for measuring rotational correlation times (τ_2) of proteins, showing the approximate time range over which each method has proven effective. Arrows indicate measurements discussed in the text.

solution to occur usually in the range from nanoseconds to microseconds. If these motions are restricted by association with other macromolecules, the characteristic times for the motions may extend to milliseconds or longer. This problem of observing rotational motions in various time ranges is illustrated in Fig. 1, in which several spectroscopic techniques are shown to indicate the time ranges in which they have proved useful in detecting rotational motions in proteins. The horizontal axis indicates the rotational correlation time (τ_2, sometimes designated τ_c or ϕ), the characteristic exponential time constant for Brownian molecular reorientation (8). The inverse of τ_2 is proportional to the rotational diffusion coefficient (Θ) and is an approximate indication of the frequency of rotational motion. (See the following discussion on rotational correlation times.) The arrows underneath the axis indicate some of the measurements discussed below. Light-scattering methods, including Raman spectroscopy, are, in principle, sensitive to correlation times over the entire time range shown, but there have been almost no measurements on proteins in the microsecond-to-millisecond time range (9–11). In addition, light-scattering often lacks the selectivity to detect a single motion in a complex system. Dielectric relaxation (12), electric dichroism (13), electric birefringence (14), and flow birefringence (15), although not shown in Fig. 1, are also sensitive to a wide range of rotational correlation times and also lack the selectivity that probes offer.

In nuclear magnetic resonance (NMR), a wide range of nuclei and methods should make it possible to detect rotational motions over a very broad time range (16). However, most reliable measurements have been made in the nanosecond range, as indicated in Fig. 1. NMR is further restricted in its usefulness by its low signal-to-noise ratio and, especially in the case of ^1H and ^{13}C, by the difficulty in selectively monitoring a single component of a complex system. Fluorescence depolarization experiments usually involve probes with lifetimes in the nanosecond range, and can achieve sensitivity to correlation times as long as hundreds of nanoseconds (17, 18). This technique is, therefore, often sensitive to rotational motions of whole proteins

and to large-scale internal motions of proteins in solution. I will discuss two applications below: (*a*) the demonstration of rotational flexibility in an antibody molecule in the range around 30 ns (19), and (*b*) the demonstration of a similar kind of flexibility in myosin that allows the myosin heads (cross-bridges) to rotate in the range around 400 ns (20–22). The conventional electron paramagnetic resonance (EPR) method, when applied to spin-labeled proteins, provides sensitivity in a similar time range, and I will discuss its use in (*a*) providing preliminary evidence for the antibody flexibility demonstrated later by fluorescence (23), and (*b*) confirming the fluorescence results on myosin (24, 25).

Until recently, there remained a gap in the range from microseconds to milliseconds in which very few measurements had been made. As mentioned above, information in this time range is essential in taking the step from isolated proteins in solution to the often more interesting situation of macromolecular assemblies, where motions are likely to be slower and more restricted. There have been efforts in several fields to extend the sensitivity to rotational motions in this time range, and there are some promising recent developments. Considerable success has been achieved with methods involving time-dependent anisotropy of the absorption or emission of long-lifetime optical probes, e.g., pyrene fluorescence (26), tryptophan phosphorescence (27), "triplet probe" absorption (28–31), and photobleaching recovery (32, 33). Another promising field is fluorescence correlation spectroscopy (18, 34).

The method I will discuss in most detail is saturation transfer spectroscopy (sometimes denoted ST-EPR), an EPR method originated by J. S. Hyde that has been used to study rotational motion of spin-labeled proteins in the range of 10^{-7} to 10^{-3} s (3, 5, 24, 25, 35–44, footnotes 1–3). I will discuss below the use of this method to (*a*) extend the study of myosin cross-bridge rotation to the slower motions occurring in supramolecular assemblies (3, 24, 25); (*b*) study flexibility within the polymeric F-actin filament (3, 24, 25, footnote 1); and (*c*) observe the rotational motions of two membrane proteins, the calcium-pumping ATPase of sarcoplasmic reticulum,[2,3] and rhodopsin (42).

Rotational Correlation Times

To understand the significance of the data from spectroscopic measurements of rotational diffusion, it is important to define precisely the rotational correlation time (8), τ_2, which characterizes the time-dependence of the orientation-dependent spectroscopic observable (e.g., the fluorescence emission anisotropy, A). The subscript "2" indicates that this spectroscopic observable, at the level of an individual molecule,

---

[1]Thomas, D. D., J. C. Seidel, and J. Gergely. 1978. Rotational dynamics of F-actin in the sub-millisecond time range. *J. Mol. Biol.*, submitted.

[2]Hidalgo, C., D. D. Thomas, and N. Ikemoto. 1978. Effect of the lipid environment on protein motion and enzymatic activity in the Ca^{2+}-ATPase of sarcoplasmic reticulum. *J. Biol. Chem.* In press.

[3]Thomas, D. D., and C. Hidalgo. 1978. Rotational motion of the Ca^{2+}-ATPase in sarcoplasmic reticulum membranes. *Proc. Natl. Acad. Sci. USA*, in press.

has the angular dependence of a spherical harmonic of order 2, for all of the techniques in Fig. 1. In the case of axial symmetry, when the observable depends only on θ, the angle between the molecular spectroscopic symmetry axis (e.g., the fluorescence emission transition moment) and the laboratory-fixed reference axis (e.g., the polarization vector of the exciting light), the angular dependence reduces to the Legendre polynomial of order 2, $P_2(\cos\theta) = \frac{1}{2}(3\cos^2(\theta) - 1)$. Then τ_2 is the exponential decay time for the autocorrelation function of P_2. That is, for an average probe molecule, the value of $\cos^2(\theta)$ after a period much greater than τ_2 has negligible correlation with the value at the beginning of the period. At the level of a large ensemble of molecules, we can measure τ_2 by selecting a population that has a nonequilibrium orientation distribution (e.g., by irradiating fluorescent probes with a flash of polarized light) and then observing the ensemble average $<P_2(\cos\theta)>$ (e.g. the fluorescence emission anisotropy, A) as it decays back to its equilibrium value. Then τ_2 is the exponential time constant of the observed decay.

Isotropic Brownian rotational diffusion corresponds to a random walk on the surface of a sphere. In this case, $<P_2(\cos\theta)>$ decays exponentially to zero, and the relationship between the observed decay time, τ_2, and the desired molecular rotational diffusion coefficient is simple: $\tau_2 = 1/(6\Theta)$. If the spectroscopic observable has the angular dependence of $P_1(\cos\theta) = \cos\theta$, as in the case of dielectric relaxation, the correlation time is $\tau_1 = 1/(2\Theta)$, as described by Debye (45, 8). Therefore, the correlation times measured by two different techniques can differ by a factor of 3 even if they correspond to the same diffusion coefficient. Since most techniques depend on $\cos^2(\theta)$ and measure τ_2, there should usually be no confusion in comparing results from different techniques. However, varying terminologies sometimes create confusion. The correlation time τ_1 in dielectric relaxation is usually called the "relaxation time" τ (12, 45). Workers in the fields of electric birefringence and electric dichroism also refer to the relaxation time τ (13, 14), even though those experiments depend on $\cos^2(\theta)$, so in this case, $\tau \equiv \tau_2 \equiv 1/(6\Theta)$. Some fluorescence workers, particularly those measuring steady-state polarization, characterize their results with the relaxation time $\rho = 1/(2\Theta)$, where $\rho \equiv 3\tau_2$, and some other fluorescence workers refer to the relaxation time $\tau = 1/(6\Theta)$.

Of course, all this confusion could be avoided if results were reported in terms of the diffusion coefficient, Θ, instead of the correlation time. However, if the rotational motion is anisotropic or restricted in angular range, the process of extracting the several Θ values from the measured τ_2 values is more difficult and usually subject to some ambiguity (46, 47). Therefore, the experimental results must often be reported as correlation (or relaxation) times, and the reader must be aware of the terminology being used. If the correlation time is determined in a steady-state experiment (e.g. EPR or steady-state fluorescence polarization), rather than by a direct time-resolved measurement of the decay of $<P_2(\cos\theta)>$, even the correlation time can be ambiguous; the effective τ_2 value estimated from the data depends on the type of motion that is assumed. For example, in a steady-state experiment it may be difficult to distinguish slow isotropic motion from rapid anisotropic motion.

FLUORESCENCE DEPOLARIZATION

As indicated above and reviewed elsewhere (17, 18, 46), fluorescence depolarization involves the selective excitation of a nonrandom orientation distribution of fluorophores by irradiation with polarized light. The emitted light is polarized also, as monitored by the emission anisotropy $A = (I_\parallel - I_\perp)/(I_\parallel + 2I_\perp)$, where $I_\parallel$ and $I_\perp$ are the emitted intensities with polarization parallel and perpendicular to that of the exciting light. This anisotropy arises because the emitting molecules have a nonrandom orientation distribution; it decreases if rotational diffusion randomizes the orientations in the period between excitation and emission. The correlation time τ_2 can be extracted indirectly from the steady-state polarization, but a less ambiguous determination of τ_2 can be obtained by directly measuring the exponential decay constant of A after a nanosecond pulse of polarized light. Since either method depends on the rotation of the fluorophore between the times of excitation and emission, τ_2 values greater than 10 fluorescence lifetimes are extremely difficult to measure. The fluorescence lifetime is typically in the range of 1–20 ns for organic fluorescent dyes.

Segmental Flexibility in Antibodies

One of the most definitive studies of large-scale rotation in proteins was the use of fluorescence depolarization to demonstrate internal flexibility in an antibody molecule, by Yguerabide et al. (19). It had been proposed that the formation of antibody-antigen complexes would be facilitated if the two heads (Fab regions, see Fig. 2) were attached by flexible joints, leaving the Fab segments free to rotate relative to each other and the Fc tail. To test this proposal, Yguerabide et al. (19), prepared IgG

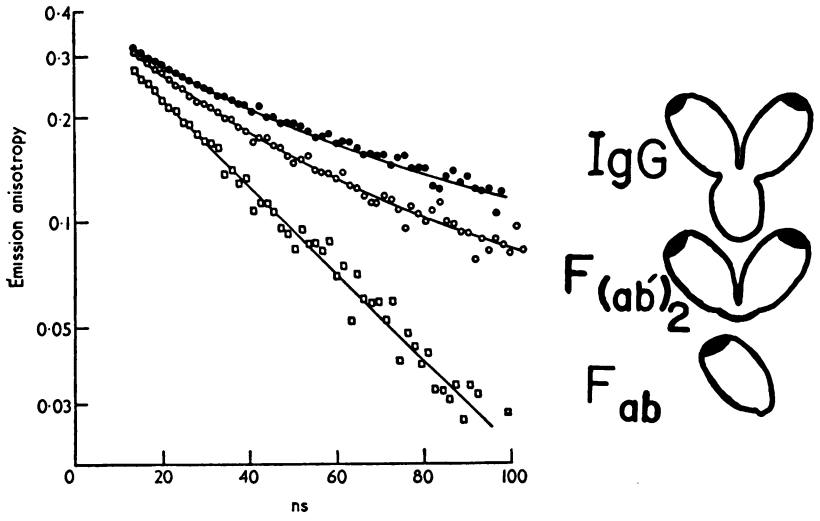

FIGURE 2 Antibody flexibility deduced from fluorescence depolarization (19). The log of fluorescence emission polarization anisotropy is plotted against time for a fluorescent hapten bound to IgG (●), F(ab')$_2$ (○), and Fab (□). See text for discussion. From Yguerabide et al. (19).

molecules that specifically bound a fluorescent hapten, dansyl cysteine, in each of the two combining regions. These workers were thus able to attach a motion-sensitive probe rigidly to the desired sites without resorting to covalent linkage. They then performed fluorescence depolarization experiments on intact IgG, on a two-headed $F(ab')_2$ fragment obtained by digestion with pepsin, and on the isolated Fab fragment obtained by digestion with papain.

The results are illustrated in Fig. 2, which shows semilogarithmic plots of the fluorescence emission polarization anisotropy vs. time. In the case of simple Brownian motion characterized by a single rotational correlation time τ_2, the slope of the curve is $-1/\tau_2$. The top curve, obtained from the intact IgG molecule, is not linear, indicating that more than one rotational correlation time contributes to the depolarization. These workers showed that the curve could be analyzed as the sum of two components, one with a τ_2 of 168 ns, a reasonable value for the overall rotation of the molecule, and another with τ_2 of 33 ns, much too short to arise from the overall motion, even if the antibody were a compact sphere. Therefore, there must be some internal flexibility in the antibody-antigen complex. To determine the site of this flexibility, these workers performed experiments on the proteolytic fragments. The $F(ab')_2$ fragment (bottom of Fig. 2) yields a single τ_2 of 33 ns. This is a time too long to allow for significant internal motion within the small Fab-antigen complex, implying that the probe is rigidly fixed to Fab, which rotates as a rigid body. The flexibility, therefore, must be at the joint between the Fab regions, as predicted.

More recently, Cathou and co-workers have extended the work of Yguerabide *et al.* (19). Holowka and Cathou (48) studied segmental flexibility in a different class of antibodies, IgM, and discussed the possible functional roles of two sites of flexibility in these molecules. Chan and Cathou (49) showed that reduction of the single inter-heavy chain disulfide of IgG increases the flexibility of the antibody. They discussed the connection between this finding and the requirement of this disulfide bond for maximal complement activation.

Segmental Flexibility in Myosin

A similar application of fluorescence depolarization, in a somewhat slower time range, was the study of segmental flexibility in myosin by Mendelson et al. (20). Myosin, the major component of the thick filament of vertebrate striated muscle, interacts with actin, the major component of the thin filaments, via an ATP-hydrolyzing "cross-bridge" containing the "head" or "S-1" (called "subfragment-1" when isolated after proteolysis) of myosin (myosin is two-headed). As illustrated schematically in Fig. 3, force generation may occur by the cyclical attachment, rotation, and detachment of cross-bridges with respect to actin, causing the filaments to slide past each other and shorten the muscle fiber (1–3). This is the proposed elementary cycle of energy transduction, in which chemical energy from ATP drives the filament motion. To test the proposal of rotational mobility of the myosin head relative to the tail, these workers attached a fluorescent iodoacetamide analogue to a specific -SH group on each head. The labeled myosin retained its ATPase activity, although the ionic dependence was

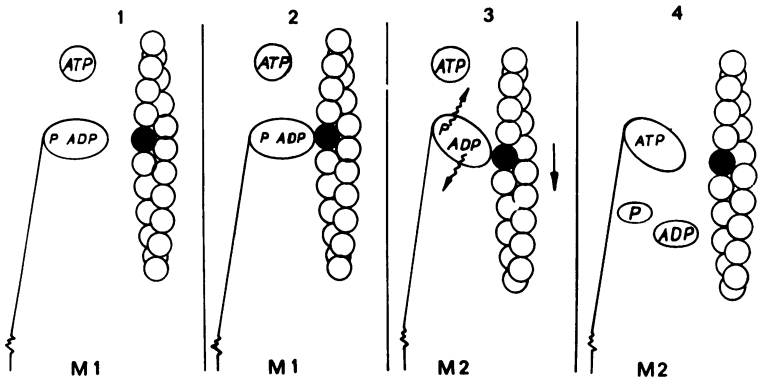

FIGURE 3 Rotating cross-bridge model for the force-generation step in muscle contraction (2). Myosin molecules are assembled into thick filaments, with their long α-helical tails forming the filament core and the globular heads (S-1) extending radially outward. For simplicity, only one myosin molecule is shown, and only one of the two heads is shown. Globular actin molecules are assembled into F-actin in double-helical thin filaments. The Ca^{2+}-regulatory thin filament proteins, troponin and tropomyosin, are not shown. The filament structures are fairly well characterized, but the following proposed molecular motions have not been demonstrated: (1 → 2) A myosin head from the thick filament forms a cross-bridge to actin on the thin filament, (2 → 3) the head rotates and propels the filaments past each other and shortens the muscle fiber (because of the bipolar filament structures), (3 → 4) the head detaches, and (4 → 1) the head rotates back, and the cycle is repeated, driven by ATP hydrolysis in the presence of Ca^{2+}. In the absence of Ca^{2+}, ATP apparently detaches the cross-bridges from actin and leaves them in state 1, so that the muscle is easily stretched (relaxation). In the absence of ATP, cross-bridges apparently remain attached in state 3, so that the muscle is resistant to stretching (rigor). From Mannherz et al. (50).

altered. The results of fluorescence depolarization experiments on the isolated molecule and its proteolytic fragments are shown in Fig. 4. As in the antibody work, the experiment on the isolated globular proteolytic fragment (subfragment-1) was crucial. The single correlation time of 2.2×10^{-7} s is several times longer than that of a sphere of the same volume; analysis (20) indicates a high probability that the probe is rigidly attached with its absorption and emission axes aligned approximately parallel to the long axis of subfragment-1, which rotates as a rigid, cigar-shaped body. The result is that the observed correlation time can be interpreted as the correlation time for reorientation of the long axis of the heads in the intact myosin molecule. In heavy meromyosin (HMM) and myosin, this correlation time is only about twice as long as in isolated subfragment-1, even though these molecules are three to four times more massive and much more aspherical than subfragment-1. As discussed by Mendelson et al. (20) these results indicate that there is flexibility within HMM, allowing the two heads (S-1) to rotate relative to the less mobile tail. Whether the two heads can rotate independently of each other is somewhat less certain, but these workers presented arguments supporting that model.

Mendelson and his colleagues also reported experiments on assemblies of proteins, and the results are shown in Fig. 5. These curves are from labeled myosin aggregated into filaments (in low ionic strength) and from labeled HMM bound to F-actin.

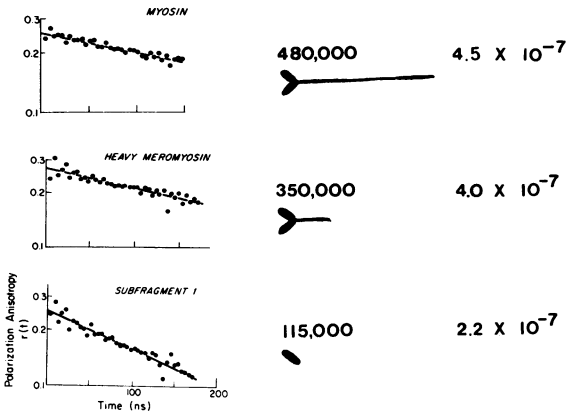

FIGURE 4

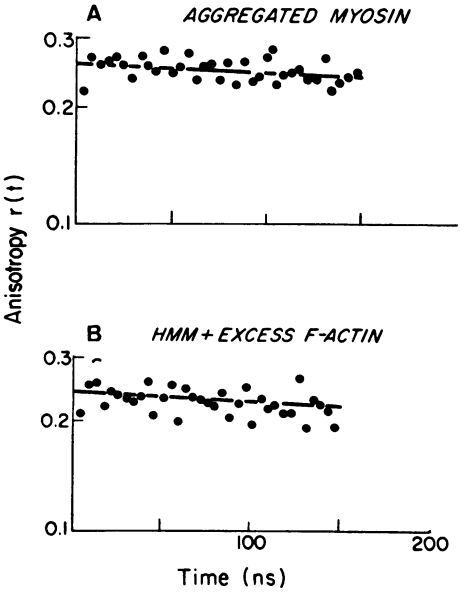

FIGURE 5

FIGURE 4 Segmental flexibility in myosin in solution at 4°C, deduced from fluorescence depolarization (20). On the left are semilogarithmic plots of fluorescence emission anisotropy vs. time, for a fluorescent dye attached to the head region of myosin and its proteolytic fragments in solution. On the right are the rotational correlation times determined from the slopes of the plots. See text for discussion. From Mendelson et al. (20).

FIGURE 5 Fluorescence depolarization data for labeled myosin heads in supramolecular assemblies (20). (A) Myosin at low ionic strength, aggregated into filaments. (B) HMM (see Fig. 4) bound to F-actin. From Mendelson et al. (20).

In each case the slopes are almost too small to measure, indicating that the τ_2 values are significantly longer than observed in the free myosin monomer (Fig. 4). It is clear that formation of these assemblies has reduced the mobility of the heads. It is, however, very difficult to estimate the τ_2 values accurately, because they are more than 10 times longer than the fluorescence lifetime. Quantitative measurements of these slower motions are important because we want to know how much flexibility persists in these more relevant assembled systems. One approach to this problem is to perform the same experiments with more time and effort devoted to improving the precision of the measurements. Mendelson and co-workers have followed this approach and have more recently succeeded in estimating τ_2 values on the order of a microsecond in myosin filaments (22). They detected a significant increase in mobility upon increasing the ionic strength or pH (confirming EPR results discussed below), but found no detectable change in mobility over the calcium concentration range known to regulate muscle contraction. They also succeeded in selectively labeling myosin heads in intact myofibrils (51, 22) but the fluorescence data (Fig. 6) indicate that the motions observed are too slow for accurate measurement by this method. The alterna-

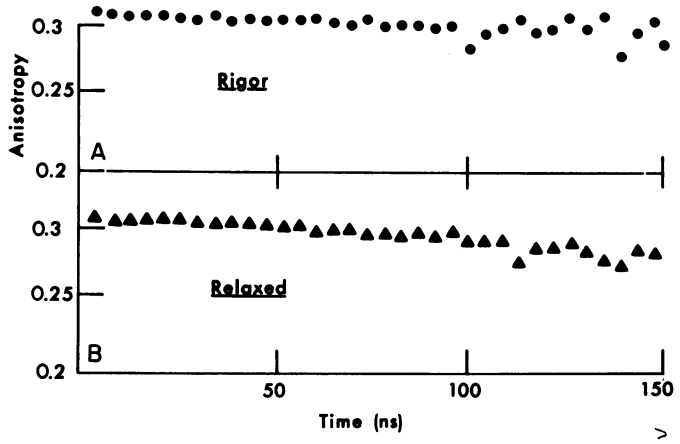

FIGURE 6 Fluorescence depolarization data from label attached to myosin heads in myofibrils (22). (A) Rigor (no ATP); (B) relaxation (during slow ATP hydrolysis in the absence of Ca^{2+}). From Mendelson and Cheung (22).

tive approach is to use a technique that, like saturation transfer EPR spectroscopy, has its maximum sensitivity to motions in the time range of interest, 10^{-7} to 10^{-3} s.

EPR

The theory and methodology of the use of nitroxide spin labels in conventional (7, 52) and saturation transfer (5, 38–40) EPR spectroscopy have been reviewed in detail elsewhere. In addition, an extensive review of saturation transfer spectroscopy by Hyde and Dalton appears in volume 2 of reference 7. Detecting rotational motions of spin labels is possible because of the anisotropic terms in the spin Hamiltonian, which make the transition energy (and the resonance Zeeman magnetic field strength) sensitive to the orientation of the spin label relative to the applied Zeeman magnetic field. To select different orientations, we vary the polarization direction in fluorescence, and the magnetic field strength in EPR. Rotational diffusion causes diffusion from one polarization to another in fluorescence, and from one Zeeman magnetic field strength to another in EPR. For technical reasons, this spectral diffusion is not observed directly in EPR, as in the time-resolved fluorescence depolarization experiment; we observe the effects of diffusion on the shape of the steady-state EPR spectrum.

Rotational correlation times are determined by comparing spectra with reference spectra obtained from experiments on model systems and from computer simulations, as shown in Figs. 7 and 8. In conventional EPR experiments (Fig. 7, left), the absorption (V) mode is detected, and a phase-sensitive detector selects the signal component oscillating in phase with the first harmonic (fundamental) of the Zeeman field modulation (usually 100 kHz), hence the designation V_1. The microwave (usually 9.5 GHz) field strength is normally kept low enough to avoid saturation; i.e., the spin system is at equilibrium and the signal amplitude increases linearly with the field strength. The resulting display is the derivative of the distribution of resonance field positions. As

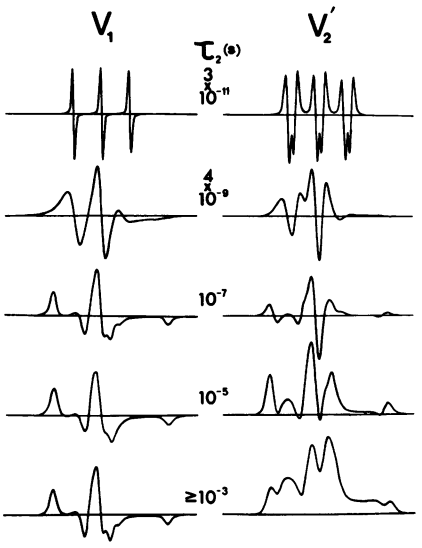

FIGURE 7 EPR reference spectra from nitroxide spin labels undergoing isotropic Brownian rotational diffusion. Conventional spectra (V_1) are on the left; saturation transfer spectra (V_2') are on the right. The correlation times (τ_2) were calculated from the viscosity, temperature, and known molecular diameters, by assuming spherical shape (38). The top pair of spectra ($\tau_2 = 3 \times 10^{-11}$ s) is from a small spin label (tempol) in aqueous solution, the second pair ($\tau_2 = 4 \times 10^{-9}$ s) is from tempol in glycerol, the third pair ($\tau_2 = 10^{-7}$ s) is from maleimide-spin-labeled hemoglobin in 40% glycerol, the fourth pair ($\tau_2 = 10^{-5}$ s) is from maleimide-spin-labeled hemoglobin in 90% glycerol, and the bottom pair ($\tau_2 \geq 10^{-3}$ s) is from maleimide-spin-labeled hemoglobin precipitated in saturated ammonium sulfate. The temperature was 20°C. The base line is 100 G wide. From Thomas (41).

the rotational correlation time becomes shorter than the inverse of the frequency resolution in the spectrum, around 10^{-7} s, the V_1 spectrum changes from the broad "rigid limit" spectrum (Fig. 7, bottom left) toward the narrow "motionally averaged" spectrum (Fig. 7, top left), resulting in good sensitivity in the time range $10^{-11} \leq \tau_2 \leq 10^{-7}$ s. However, sensitivity is poor for $\tau_2 > 10^{-7}$ s.

The most essential difference in the saturation transfer method (38) is that the microwave field strength is increased to a partially saturating level; i.e., the spin system is no longer at equilibrium and the V_1 signal amplitude increases less than linearly with the field strength. Since rotational motion can transfer spins between the irradiated (saturated) point and another point in the spectrum, rotational motion can transfer saturation away from resonance. If this transfer occurs within a time comparable to the intrinsic spin-lattice relaxation time T_1 (the exponential time constant for the dissipation of saturation), then the effects of saturation on the spectrum are reduced. Since T_1 is approximately 10^{-5} s, and since only a rotation of a few degrees is required for an effective transfer of spins, effects on the spectrum should be observed for correlation times as long as 10^{-3} s.

However, the shapes of V_1 spectra are affected only slightly by moderate saturation,

so only slight spectral changes occur when rotational motion reduces the saturation effects. Spectral displays more sensitive to saturation transfer can be obtained by other detection schemes; e.g., U_1' (dispersion mode, first harmonic, out-of-phase). The most direct, but experimentally most difficult, method is electron-electron double resonance (ELDOR). The detection method most often used in biophysical studies yields the spectra shown at the right in Fig. 7. In these experiments, the Zeeman field is modulated at 50 kHz, but the phase-sensitive detector selects the signal component oscillating at 100 kHz, the second harmonic of the modulation frequency. If the in-phase component is selected, the spectrum is designated V_2. To obtain the V_2' spectrum, the component oscillating 90° out of phase is selected. In the absence of saturation, the V_2' signal is extremely weak, but at microwave field strengths sufficient to cause saturation, the absorption lags behind the field modulation. The out-of-phase signal, V_2', becomes large when the modulation frequency, ω_m, becomes comparable to (or greater than) the relaxation rate, T_1^{-1}. The resulting signal is almost totally due to saturation, and is very sensitive to saturation transfer, which reduces the signal amplitude. At some spectral positions, rotational motion causes more saturation transfer than at other positions (38). Therefore, rotational motion reduces the signal

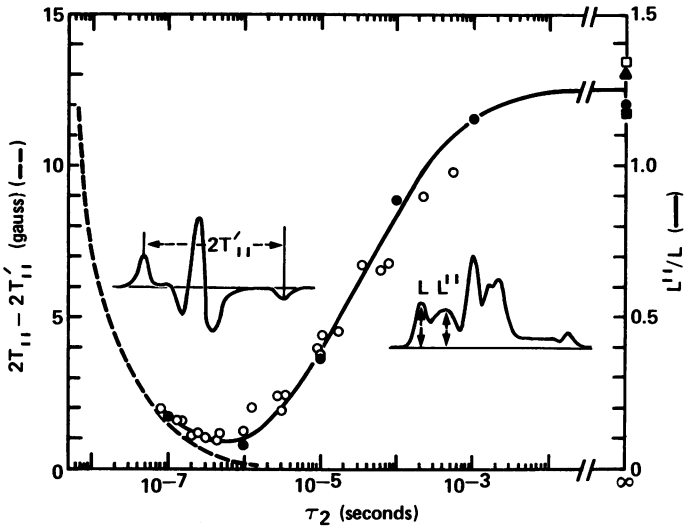

FIGURE 8 Parameters from conventional (V_1) and saturation transfer (V_2') EPR spectra of nitroxide spin labels, undergoing isotropic rotational diffusion at correlation time τ_2. The broken curve (scale at left) is from computer simulations of conventional (V_1) spectra (52). $T_{||}$ is the value of the electron-nuclear hyperfine interaction when the nitroxide principal axis is parallel to the DC magnetic field, and $2T_{||}$ is the observed separation of the outer extrema for a randomly oriented, immobilized ensemble. $2T_{||}'$ is the observed separation (see inset), so the left ordinate is the decrease in this separation due to rotational motion. The solid curve (scale at right) is from computer-simulated (•) and experimental (○) saturation transfer (V_2') spectra (37, 38). Open symbols are from maleimide-spin-labeled hemoglobin (Fig. 7). At $\tau_2 = \infty$, the closed square is from crystallized hemoglobin, and the closed triangle is from a 100,000 = g pellet of maleimide-spin-labeled actin.

amplitude at some positions (e.g. peak L'' in Fig. 8) more than others (e.g. peak L in Fig. 8), changing the shape of the spectrum. As τ_2 becomes shorter than 10^{-3} s, the V_2' spectrum changes from the rigid limit spectrum, shaped like the integral of V_1 (Fig. 7, bottom right), toward a spectrum shaped like the derivative of V_1 (Fig. 7, center right). Fig. 8 shows plots of spectral parameters vs. τ_2 for both EPR methods, and demonstrates the agreement between saturation transfer experiments and theory. It should be noted that, although the peak ratio L''/L (Fig. 8) is useful only for measuring correlation times longer than 10^{-6} s, the center of the spectrum is also sensitive to correlation times from 10^{-8} to 10^{-5} s (38). Therefore, the two EPR methods can be used to measure correlation times in the entire range $10^{-11} \leq \tau_2 \leq 10^{-3}$ s.

Segmental Flexibility in Antibodies

Although the fluorescence depolarization work of Yguerabide, et al. (19) has provided the most important evidence for antibody flexibility, Stryer and Griffith used a spin-labeled hapten several years earlier to obtain preliminary evidence for this flexibility (23). They prepared a dinitrophenyl nitroxide that was combined with anti-dinitrophenyl antibody, and they estimated the rotational correlation time from the conventional EPR spectrum. Their measured rotational relaxation time (ρ) of 35 ns corresponds to a rotational correlation time (τ_2) of 12 ns. This time is much shorter than expected for the overall motion, so it is consistent with segmental flexibility. However, the possibility of nonrigid binding or internal motion within the probe itself was not ruled out. Spin-labeled haptens and covalently attached spin labels have been used in a number of other studies of antibody flexibility, as reviewed recently by Käiväräinen and Nezlin (53).

Segmental Flexibility in Myosin

My co-workers and I spin-labeled the head region of myosin with an iodoacetamide analogue to extend the measurement of cross-bridge rotation to correlation times

TABLE I

DEMONSTRATION OF SEGMENTAL FLEXIBILITY IN MYOSIN IN SOLUTION BY EPR (24, 25) AND FLUORESCENCE (20)

	Conventional EPR		Saturation transfer		Fluorescence depolarization	
	$\tau_2 \times 10^7$	$\frac{\tau_2}{\tau_2(\text{S-1})}$	$\tau_2 \times 10^7$	$\frac{\tau_2}{\tau_2(\text{S-1})}$	$\tau_2 \times 10^7$	$\frac{\tau_2}{\tau_2(\text{S-1})}$
S-1	1.6		2.2		2.2	
HMM	2.15	1.3	3.2	1.5	4.0	1.8
Myosin	2.5	1.6	3.7	1.7	4.5	2.0

Data are from subfragment – 1(S-1), HMM, and myosin monomers. Correlation times are given in seconds. The absolute correlation times are not directly comparable, because the EPR experiments were performed at 20°C, the fluorescence at 4°C. τ_2/τ_2 (S-1) is the ratio of the observed correlation time to that of S-1. See text for discussion.

$>10^{-6}$ s (24, 25). As in the fluorescence work, the labeled myosin retained its ATPase activity. We performed EPR experiments on myosin and its proteolytic fragments and determined τ_2 from conventional EPR, by measuring the parameter $2T'_{||}$ (Fig. 8), and from saturation transfer EPR, by observing the central region of the spectrum. The results are similar to those of the fluorescence work discussed above, as summarized in Table I. All three techniques—conventional EPR, saturation transfer EPR, and fluorescence depolarization—yield (*a*) much longer correlation times for subfragment-1 than expected for a rigid sphere of the same volume, and (*b*) ratios τ_2/τ_2(S-1) for myosin and heavy meromyosin that are 2.0 or less. Like the iodoacetamide fluorophore, the iodoacetamide spin label is rigidly attached and appears to report the correlation time of the long axis of the myosin head; the earlier finding of segmental flexibility in myosin monomers is confirmed.

Our main purpose was to study this flexibility in supramolecular assemblies where conditions are more like those in a muscle fiber, but where the motions are too slow for accurate measurement by fluorescence depolarization. Fig. 9 summarizes some of the results of this work (3, 24, 25). On the right are the myosin spectra, and on the left are model system reference spectra for comparison. The conventional (V_1) spectra (not shown) showed almost no changes due to the formation of these assemblies, indicating that the label remains rigidly bound and that the changes observed in the saturation transfer spectra must be due to changes in slow (presumably large-scale) rotational motions. When myosin in 0.5 M KCl, where it is monomeric (Fig. 9 E), is dialyzed against lower ionic strength buffer, it assembles into filaments similar in appearance (in electron micrographs) to the thick filaments of muscle. At 0.137 M KCl, pH 8.3, these filaments are somewhat smaller and less ordered than native thick filaments, and they produce spectrum 9D, indicating a correlation time several times longer than that found in myosin monomers. We found that decreasing either the ionic strength or pH increases the correlation time further, a result confirmed by fluorescence work (22). But even at 0.025 M KCl, pH 7.0 (Fig. 9 C), where the filaments form visible aggregates, the correlation time is $<10^{-5}$ s. In each case the correlation time observed in synthetic myosin filaments is at least 10 times shorter than any correlation time possible for the entire assembly. The additional motion is probably due to rotation of myosin heads. Thus, over a wide range of ionic conditions, the motion of heads in myosin filaments is restricted relative to that observed in monomers, but the myosin heads retain significant rotational mobility in the microsecond time range. This motion is easily fast enough to be consistent with the rotating cross-bridge model of muscle contraction (Fig. 3). At present, our ability to analyze the spectra in terms of the geometric details of the motion is quite limited. Thus, it is possible that some of the apparent increase in correlation time upon filament formation is due to a restriction in the angular range of myosin head rotation, as suggested by Mendelson and Cheung (22), and not only to a slowing down of the same motion observed in myosin monomers.

A much more dramatic change is observed when an excess of F-actin (a model for the thin filament) is added to myosin monomers (Fig. 9 A): τ_2 increases by a factor of

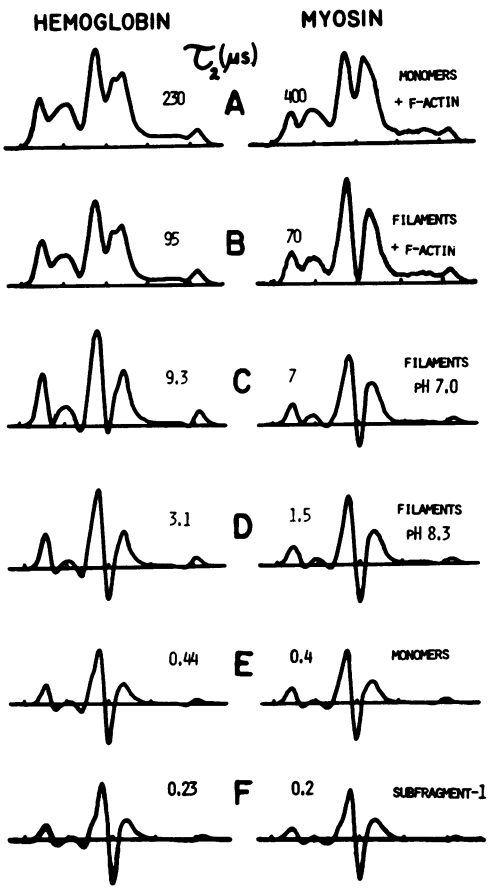

FIGURE 9 Saturation transfer EPR spectra of iodoacetamide-spin-labeled myosin and its derivatives (right), at 20°C (3, 24, 25). τ_2 is the rotational correlation time. The spectra on the left are for comparison and were obtained from maleimide-spin-labeled hemoglobin in glycerol-water solutions (Fig. 7). The τ_2 values for the myosin samples were determined by comparing their spectra with hemoglobin spectra and with theoretically simulated spectra, using spectral parameters such as L''/L (Fig. 8). Spectra are from (F) subfragment-1 in solution, (E) myosin monomers in solution (0.5 M KCl), (D) myosin filaments in 0.137 M KCl, 0.02 M Tris, pH 8.3, (C) myosin filaments in 0.03 M KCl, 0.02 M Tris, pH 7.0, (B) myosin filaments (from D) plus excess F-actin, and (A) myosin monomers (from E) plus excess F-actin. From Thomas et al (3).

1,000, to a point near the limit of sensitivity for even the saturation transfer method. These are conditions where myosin heads form rigor cross-bridges with actin. It is clear that this complex with actin strongly immobilizes both S-1 regions (heads) of myosin and that the actin-S-1 rigor complex is a rigid unit. A rigid linkage between the myosin head and actin may be important in the efficient generation of force. If the joint between the two heads remains flexible, the immobilization of both heads implies that both are bound to actin. Fig. 9 B shows that F-actin also immobilizes myosin heads in myosin filaments, i.e., at low ionic strength. Note, however, that the

degree of immobilization is less than at high ionic strength (Fig. 9 A). The most probable explanation is that steric constraints in the mixture of unoriented thick and thin filaments make it difficult for every myosin head to bind to an actin monomer. The resulting spectrum (Fig. 9 B) contains some contribution from unattached heads (Fig. 9 D) as well as a contribution from attached heads (Fig. 9 A).

Further progress in understanding the rotational dynamics of myosin heads requires that we make measurements under conditions that more closely resemble muscle contraction. One factor that has slowed progress is that the iodoacetamide spin label, used to label myosin in the work described above, does not remain rigidly immobilized on the myosin head during ATP hydrolysis; i.e., large changes are observed in the conventional EPR spectrum. We have recently solved this problem by labeling myosin with a maleimide spin label, followed by treatment with ferricyanide, as suggested by P. Graceffa (Boston Biomedical Research Institute). This label remains rigidly bound during ATP hydrolysis, i.e., ATP causes no change in the conventional (V_1) spectrum. In addition, we have succeeded in labeling myosin heads with this maleimide derivative in intact myofibrils and in whole glycerinated muscle fibers by a procedure similar to that used to label fibers with fluorescent dyes (22). The results of preliminary saturation transfer experiments on these maleimide-spin-labeled myofibrils indicate that (*a*) myosin heads rotate in the sub-millisecond time range in synthetic thick filaments, (*b*) ATP has no effect on this motion, and (*c*) a similar (but slightly slower) motion, in the sub-millisecond time range, is observed in relaxed myofibrils (5 mM MgATP, 1 mM EGTA) and in contracting myofibrils (5 mM MgATP, 0.1 mm $CaCl_2$), but the motion stops when the ATP is used up (rigor). These are the first direct observations of cross-bridge rotational motion during contraction. This work shows the power of spectroscopic probes in detecting selected motions in complex systems.

Rotational Dynamics in Actin Filaments

Since force-generation involves the dynamic interaction of thick (myosin-containing) and thin (actin-containing) filaments, it seemed worthwhile to investigate the molecular dynamics of the actin filament (3, footnote 1). The dynamic state of actin may be crucial in the interaction of actin and myosin in muscle; it may be even more important in the contractile assemblies found in nonmuscle cells, where actin is the predominant contractile protein and it appears that the regulation of actin's supramolecular state is more complex than in muscle (54). We have spin-labeled actin with a maleimide analogue that appears to bind quite rigidly with an orientation that makes the label sensitive primarily to bending motions; that is, changes in the orientation of the filament axis (55). The saturation transfer spectrum of spin-labeled F-actin at 20°C (Fig. 10, top right) yields an effective correlation time of 10^{-4} s. Evidence has been previously reported, from light-scattering experiments (56–58), for F-actin bending motions in the time range around 10 ms, corresponding to changes in the end-to-end distance of the entire filament. The motions reported by the spin label in the sub-

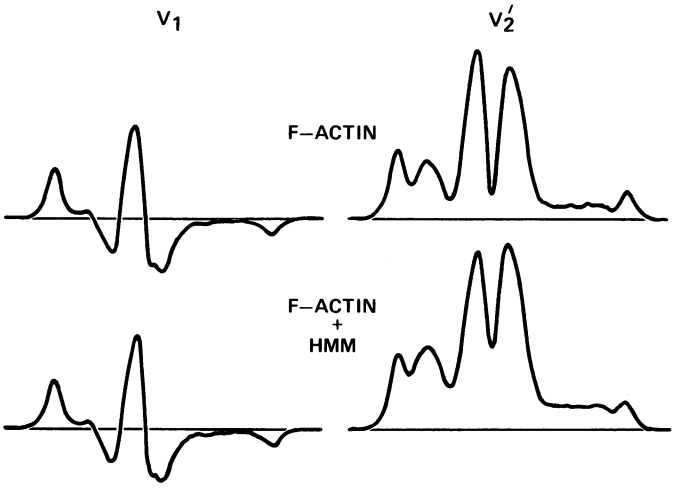

FIGURE 10 Conventional (V_1, left) and saturation transfer (V_2', right) EPR spectra obtained from malemide-spin-labeled F-actin (top) and from labeled F-actin plus 0.1 mol HMM/mol of actin monomer (bottom), at 20°C (3).[1] From Thomas et al.[1]

millisecond time range probably correspond to a more localized scale than the motions affecting the light-scattering results.

As Fig. 10 shows, the addition of HMM to actin increases the peak ratio L''/L, indicating slower motion within the actin filament. Note that the conventional spectrum is essentially unchanged. Myosin and subfragment-1 have similar effects (3, footnote 1). The immobilization of F-actin by myosin heads is highly cooperative; that is, only about 0.1 molecule of myosin, HMM, or S-1 per binding site (actin monomer) is required to achieve a maximal effect, as shown in Fig. 11 for HMM. This finding adds to the physical and biochemical evidence that the effects of the binding of myosin heads can be propagated along the actin filament even in the absence of the regulatory proteins tropomyosin and troponin (57–61).

Rotational Mobility of Membrane Proteins

An important example of large-scale protein motion in macromolecular assemblies is the rotational motion of membrane proteins, and a number of studies have recently been carried out in this field (32, 33, 30, 42, 43, 62, footnotes 2 and 3). Optical spectroscopic techniques have yielded some of the first direct measurements of rotation of membrane proteins. Cone (32) measured a correlation time of 4 ± 2 μs for the rotation of rhodopsin about an axis perpendicular to the plane of the disk membrane of the rod outer segment in an intact retina, by observing the decay of dichroism after the bleaching (with a polarized flash) of the intrinsic chromophore, 11-cis-retinal. Cherry et al. (30) observed the flash-induced dichroism of a covalently attached triplet probe (eosin isothiocyanate) to detect rotational motion in the millisecond range for the "band 3" proteins of human erythrocyte membranes.

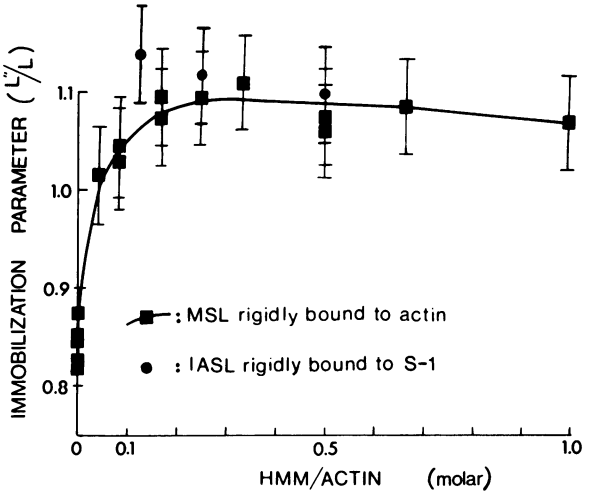

FIGURE 11

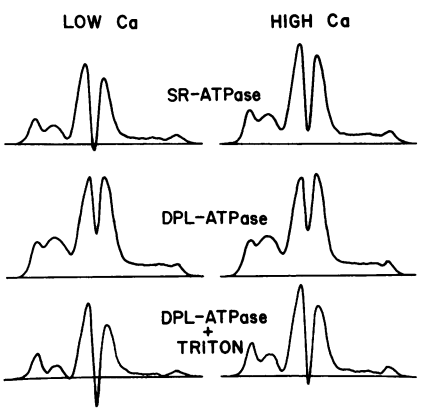

FIGURE 12

FIGURE 11 The dependence of L''/L, a parameter from saturation transfer EPR spectra (Fig. 8), on the mole ratio of HMM to F-actin (3).[1] As indicated, squares are from experiments in which the spin label was on actin, and circles are from experiments in which the label was on the head (S-1 region) of HMM. The value of L''/L corresponding to no detectable motion (obtained from a pellet of spin-labeled actin; Fig. 8) is 1.30. From Thomas et al. (3).

FIGURE 12 Saturation transfer EPR spectra obtained from a maleimide spin label attached to the Ca^{2+}-ATPase from SR, at 4°C.[2,3] Top: SR-ATPase, a preparation containing endogeneous SR lipids. Center: DPL-ATPase, in which dipalmitoyl lecithin (DPL) has been substituted for the endogenous lipids. Bottom: DPL-ATPase, after the addition of the detergent Triton X-100, at a ratio of 1.5 mg/mg protein. Left: 10^{-5} M Ca^{2+}. Right: 10^{-2} M Ca^{2+}. From Hidalgo et al.[2]

Devaux and his co-workers have carried out saturation transfer studies on several membrane-bound proteins, including rhodopsin (from retinal rod outer segments), the acetyl choline receptor (from *Torpedo* electric organs), and a mitochondrial ADP carrier (42–44). The results of experiments with maleimide-spin-labeled rhodopsin by Baroin et al. (42) indicate that this membrane protein rotates in the microsecond time range at room temperature, and this motion stops when the proteins are cross-linked with glutaraldehyde. These results are in good agreement with those of Cone (32). At 20°C, the effective correlation time from EPR is 15–20 μs (42). This value is several times longer than that observed by Cone. This difference is expected, since the EPR experiment measures a time-average in a suspension of randomly oriented membranes, so that the time-resolved motion observed by Cone about a single axis in oriented membranes becomes averaged with slower motions about other axes in the EPR experiments. Although Cone's results applied only to the motion of previously unbleached rhodopsin during a period of several microseconds after excitation, the EPR results were obtained for both bleached and unbleached rhodopsin, and revealed no difference in protein mobility between the two states. Therefore, it is unlikely

that light-dependent aggregation of rhodopsin molecules plays a role in visual excitation.

My co-workers and I have carried out studies of the Ca^{2+}-ATPase of sarcoplasmic reticulum (SR) membranes using saturation transfer spectroscopy.[2,3] To investigate the roles of the motional states of protein and lipid in enzyme action, we applied various perturbations to the membrane system and then correlated the observed changes in ATPase activity with changes in lipid fluidity (monitored by EPR spectra of a stearic acid spin label) and protein rotational mobility (monitored by EPR spectra of the spin-labeled enzyme polypeptide). We attached a maleimide spin label selectively and rigidly to the enzyme, and obtained a preparation with only slightly decreased ATPase activity. Saturation transfer (V_2') spectra from preparations containing the spin-labeled Ca^{2+}-ATPase at 4°C are shown in Fig. 12. The corresponding conventional (V_1) spectra (not shown) are all virtually identical and indicate that the labels are strongly immobilized. Therefore, any observed differences in V_2' spectra are due to slow, presumably large-scale, rotational motion, probably corresponding to rotation of the whole enzyme or a large segment of it. The spectrum of the purified Ca^{2+}-ATPase in vesicles of endogenous SR lipids (SR-ATPase), at 4°C in 10^{-5} M Ca^{2+}, yields a value of $L''/L = 0.74 \pm 0.02$, corresponding to an effective correlation time of $\tau_2 = 6 \times 10^{-5}$ s (Fig. 12, top left). This is approximately twice the τ_2 value obtained at 4°C for spin-labeled rhodopsin (42), suggesting that the effective viscosities are similar in the two membranes. The addition of 10 mM $CaCl_2$, which inhibits the enzyme by preventing phosphate-release after ATP hydrolysis, decreases the enzyme's rotational mobility (Fig. 12, top right: $L''/L = 0.85 \pm 0.02$, $\tau_2 = 1.1 \times 10^{-4}$ s). When the relatively fluid SR lipids are replaced with the completely saturated phospholipid dipalmitoyl lecithin (DPL), the resulting DPL-ATPase preparation has a rigid lipid phase at 4°C (63), the phosphate-release step is again strongly inhibited (63), and the protein's rotational motion is markedly slowed, both at 10^{-5} and 10^{-2} M Ca^{2+} (Fig. 12, center). The value of $L''/L = 1.13 \pm 0.01$ is at or near the limit of sensitivity for saturation transfer, implying that the correlation time is on the order of 10^{-3} s or longer. The addition of Triton X-100 to DPL-ATPase dissolves the membrane, restores the ATPase activity, and increases greatly the rotational mobility of the enzyme (Fig. 12, bottom left: $L''/L = 0.51 \pm 0.02$, $\tau_2 = 2 \times 10^{-5}$). Even in the absence of a phospholipid bilayer, 10 mM $CaCl_2$ inhibits the enzyme and slows the rotational motion (Fig. 12, bottom right: $L''/L = 0.64 \pm 0.02$, $\tau_2 = 4 \times 10^{-5}$).

In summary, these experiments show a consistent correlation between enzymatic activity and the rotational mobility of the protein, indicating that the efficient functioning of this transport enzyme may require that the protein be free to rotate in the sub-millisecond time range. The requirement of protein mobility for transport activity has been proposed previously (4, 5, 64, 65), but this work is the first demonstration of a correlation between enzyme activity and direct measurements of rotational motion. We do not yet know the geometric details of the observed rotational motion. However, this transport enzyme can function even if antibodies are bound to the

protein, presumably preventing a 180° rotation about an axis in the plane of the membrane (66, 67). It is likely, therefore, that any essential large-angle rotations are about an axis perpendicular to the membrane plane, as is probably the case for rhodopsin (32).

It is important to note that, in both ST-EPR studies of enzyme motion (on cross-bridges and on SR), the observed rates of protein rotation (as estimated by $1/\tau_2$) are much faster than the enzyme cycling rates, and there are cases where these motions occur even in the absence of substrate. However, the enzymes only function when they are rotationally mobile. Therefore, although the data are consistent with models in which the observed rotational motions are required for enzyme function, these motions are not tightly coupled to the enzymatic cycle.

Other Applications of ST-EPR

Dalton and his co-workers, who have made major contributions to the theory of saturation transfer, have begun a number of studies on protein assemblies using saturation transfer spectroscopy (39, 68, footnote 4). One of these is the study of the kinetics of aggregation of hemoglobin S from sickle cell patients.[4] Another is the study of erythrocyte membranes from muscular dystrophy patients (68). It was found that the saturation transfer technique was sensitive to disease-associated changes that were not detected by conventional EPR. Hemminga et al. (69), applied ST-EPR to the study of a tobacco mosaic virus protein. These and other applications of saturation transfer spectroscopy are discussed in a recent review by Hyde (40).

DISCUSSION

It should be noted that the correlation times determined in the saturation transfer experiments described above are based on comparison with spectra from isotropically tumbling spin labels (Figs. 7, 8). Because many of the actual motions, particularly those of membrane proteins, are likely to be anisotropic, these estimated correlation times cannot be taken as accurately describing the details of the molecular motions. More detailed information will be available when (*a*) spectra corresponding to anisotropic motions are simulated theoretically and (*b*) experiments are performed on uniformly oriented samples, e.g., parallel muscle fibers or parallel membrane planes. In general, time-resolved experiments, like those described above involving anisotropic absorption or emission by optical probes, are most likely to provide unambiguous information about complex motions or motions in a heterogeneous system (46, 70). An ideal method might be time-resolved ST-EPR (that is, a pulsed electron-electron double resonance experiment), since EPR spectra provide more detailed orientation information than optical spectra. However, in the two cases where both saturation transfer EPR and time-resolved optical spectroscopy have been used, (*a*) in observing the motion of the heads of myosin monomers in solution (20, 24), and (*b*) in observing

[4]Lionel, T., M. E. Johnson, and L. R. Dalton. 1978. Hb self-aggregation kinetics as monitored by ST-EPR. Manuscript in preparation.

the extremely anisotropic rotation of rhodopsin (32, 42), the two methods yield very nearly the same correlation times.

The interpretation of spectroscopic data in terms of molecular dynamics almost always involves some important assumptions and, consequently, some ambiguity. The use of more than one technique, as in several of the examples cited above, establishes the conclusions much more firmly. It appears likely that a variety of magnetic resonance and optical spectroscopic techniques will continue to provide crucial information about large-scale rotational dynamics of proteins, helping to elucidate molecular mechanisms in increasingly complex biological processes.

I am grateful to John Gergely, Lubert Stryer, Harden McConnell, Robert Mendelson, James Hyde, and Philippe Devaux for helpful comments and data.

This work was supported by the Muscular Dystrophy Associations of America and a Helen Hay Whitney Foundation fellowship.

Received for publication 1 February 1978 and in revised form 19 June 1978.

REFERENCES

1. HUXLEY, A. F. 1957. Muscle structure and theories of contraction. *Progr. Biophys. Biophys. Chem.* **7**:255–318.
2. HUXLEY, H. E. 1969. The mechanism of muscular contraction. *Science (Wash. D. C.).* **164**:1356–1366.
3. THOMAS, D. D., J. C. SEIDEL, and J. GERGELEY. 1976. Molecular motions and the mechanism of muscle contraction and its regulation. *In* Contractile Systems in Non-Muscle Tissues. S. V. Perry, A. Margreth, and R. S. Adelstein, editors. Elsvier/North-Holland, Inc., New York. 13–21.
4. MCCONNELL, H. M., C. F. FOX, and G. L. NICHOLSON. 1975. Lateral molecular motions in membranes. *In* Functional Linkage in Biomolecular Systems. F. O. Schmitt, D. M. Schneider, and D. M. Crothers, editors. Raven Press, New York. 123–147.
5. MCCONNELL, H. M. 1976. Molecular Motion in Biological Membranes. *In* Spin Labeling, Theory and Applications. L. J. Berliner, editor. Academic Press, Inc., New York. 525–560.
6. KIRTLEY, M. D., and D. E. KOSHLAND, JR. 1972. Environmentally sensitive groups attached to proteins. *Methods Enzymol.* **26**:578–601.
7. BERLINER, L. J., editor. 1976. Spin Labeling, Theory and Applications. Academic Press, Inc., New York. 592 p.
8. CARRINGTON, A., and A. D. MCLACHLAN. 1967. Introduction to Magnetic Resonance. Harper & Row, New York. 187–189, 259–260.
9. CARLSON, F. D. 1975. The application of intensity fluctuation spectroscopy to molecular biology. *Annu. Rev. Biophys. Bioeng.* **4**:243–264.
10. BERNE, B. J., and R. PECORA. 1976. Dynamic Light Scattering. John Wiley & Sons, Inc., New York. 376 pp.
11. SCHURR, J. M. 1976. Relaxation of rotational and internal modes of macromolecules determined by dynamic scattering. *Q. Rev. Biophys.* **9**:109–134.
12. TAKASHIMA, S. 1969. Dielectric properties of proteins. I. Dielectric relaxation. *In* Physical Principles and Techniques of Protein Chemistry, Part A. S. J. Leach, editor. Academic Press, Inc., New York. 291–333.
13. PAULSON, C. M., JR. 1976. Electric dichroism of macromolecules. *In* Molecular Electro-optics, Part 1, Theory and Methods. C. T. O'Konski, editor. Marcel Dekker, Inc., New York. 243–274.
14. O'KONSKI, C. T. 1976. Electric birefringence and relaxation in solutions of rigid macromolecules. *In* Molecular Electro-optics, Part 1, Theory and Methods. C. T. O'Konski, editor. Marcel Dekker, New York. 63–120.
15. TANFORD, C. 1961. Physical Chemistry of Macromolecules. John Wiley & Sons, Inc., New York. 437–447.

16. DWEK, R. A. 1973. NMR in Biochemistry. Clarendon Press, Oxford, U.K. 395 p.
17. YGUERABIDE, J. 1972. Nanosecond fluorescence spectroscopy of macromolecules. *Methods Enzymol.* **26**:498–578.
18. RIGLER, M. 1977. Fluorescence relaxation and correlation spectroscopy in the analysis of conformational dynamics. *Trends Biochem. Sci.* **2**:252–254.
19. YGUERABIDE, J., H. F. EPSTEIN, and L. STRYER. 1970. Segmental flexibility in an antibody molecule. *J. Mol. Biol.* **51**:573–590.
20. MENDELSON, R. A., M. F. MORALES, and J. BOTTS. 1973. Segmental flexibility of the S-1 moiety of myosin. *Biochemistry.* **12**:2250–2255.
21. MENDELSON, R. A., S. PUTNAM, and M. F. MORALES. 1975. Time-dependent fluorescence depolarization and lifetime studies of myosin subfragment-one in the presence of nucleotide and actin. *J. Supramol. Struct.* **3**:162–168.
22. MENDELSON, R. A., and P. CHEUNG. 1976. Muscle crossbridges: absence of a direct effect of calcium on movement away from the thick filaments. *Science (Wash. D. C.).* **194**:190–192.
23. STRYER, L., and O. H. GRIFFITH. 1965. A spin-labeled hapten. *Proc. Natl. Acad. Sci. U. S. A.* **54**: 1785–1791.
24. THOMAS, D. D., J. C. SEIDEL, J. S. HYDE, and J. GERGELY. 1975. Motion of subfragment-1 in myosin and its supramolecular complexes: saturation transfer electron paramagnetic resonance. *Proc. Natl. Acad. Sci. U. S. A.* **72**:1729–1733.
25. THOMAS, D. D., J. C. SEIDEL, J. GERGELY, and J. S. HYDE. 1975. The quantitative measurement of rotational motion of the subfragment-1 region of myosin by saturation transfer EPR spectroscopy. *J. Supramol. Struct.* **3**:376–390.
26. WELTMAN, J. K., R. P. SZARO, A. R. FRANKELTON, JR., R. M. DOWBEN, J. R. BUNTING, and R. E. CATHOU. 1973. N-(3-pyrene maleimide: a long lifetime fluorescent sulfhydryl reagent. *J. Biol. Chem.* **248**:3173–3177.
27. STRAMBINI, G., and W. C. GALLEY. 1976. Detection of slow rotational motions of proteins by steady-state phosphorescence anisotropy. *Nature (Lond.).* **260**:554–556.
28. CHERRY, R. J., A. COGOLI, M. OPPLIGER, G. SCHNEIDER, and G. SEMENZA. 1976. A spectroscopic technique for measuring slow rotational diffusion of macromolecules. 1. Preparation and properties of a triplet probe. *Biochemistry.* **15**:3653–3656.
29. CHERRY, R. J., and G. SCHNEIDER. 1976. A spectroscopic technique for measuring slow rotational diffusion of macromolecules. 2. Determination of rotational correlation times of proteins in solution. *Biochemistry.* **15**:3657–3661.
30. CHERRY, R. J., A. BÜRKLI, M. BUSSLINGER, G. SCHNEIDER, and G. R. PARRISH. 1976. Rotational diffusion of band 3 proteins in the human erythrocyte membrane. *Nature (Lond.).* **263**:389–393.
31. LAVALETTE, D., B. AMAND, and F. POCHON. 1977. Rotational relaxation of 70S ribosomes by a depolarization method using triplet probes. *Proc. Natl. Acad. Sci. U.S.A.* **74**:1407–1411.
32. CONE, R. A. 1972. Rotational diffusion of rhodopsin in the visual receptor membrane. *Nat. New Biol.* **236**:39–43.
33. JUNGE, W., and U. KUNZE. 1977. Ellipticity of cytochrome a_3 and rotational mobility of cytochrome c-oxidase in the cristae membrane of mitochondria. *FEBS (Fed. Eur. Biochem. Soc.) Lett.* **80**:429–434.
34. EHRENBERG, M., and R. RIGLER. 1976. Fluorescence correlation spectroscopy applied to rotational diffusion of macromolecules. *Q. Rev. Biophys.* **9**:69–81.
35. HYDE, J. S., and L. R. DALTON. 1972. Very slowly tumbling spin labels: adiabatic rapid passage. *Chem. Phys. Lett.* **16**:508–572.
36. HYDE, J. S., and D. D. THOMAS. 1973. New EPR methods for the study of very slow motion: application to spin-labeled hemoglobin. *Ann. N. Y. Acad. Sci.* **222**:680–692.
37. THOMAS, D. D., and H. M. MCCONNELL. 1974. Calculation of paramagnetic resonance spectra sensitive to very slow rotational motion. *Chem. Phys. Lett.* **25**:470–475.
38. THOMAS, D. D., L. R. DALTON, and J. S. HYDE. 1976. Rotational diffusion studied by passage saturation transfer electron paramagnetic resonance. *J. Chem. Phys.* **65**:3006–3024.
39. DALTON, L. R. 1976. Saturation transfer spectroscopy. *Adv. Magn. Resonance.* **8**:149–259.
40. HYDE, J. S. 1978. Saturation transfer spectroscopy. *Methods Enzymol.* **49**:480–511.
41. THOMAS, D. D. 1977. Saturation transfer EPR. *Trends Biochem. Sci.* **2**:N62–N63.

42. BAROIN, A., D. D. THOMAS, B. OSBORNE, and P. DEVAUX. 1977. Saturation transfer electron paramagnetic resonance on membrane-bound proteins. I—rotational diffusion of rhodopsin in the visual receptor membrane. *Biochem. Biophys. Res. Commun.* **78**:442–447.
43. ROUSSELET, A., and P. F. DEVAUX. 1977. Saturation transfer electron paramagnetic resonance on membrane-bound proteins. II—absence of rotational diffusion of the cholinergic receptor protein in torpedo marmorata membrane fragments. *Biochem. Biophys. Res. Commun.* **78**:448–454.
44. DEVAUX, P. F., A. BAROIN, A. BIENVENUE, E. FAVRE, A. ROUSSELET, and D. D. THOMAS. 1978. Rotational diffusion of various membrane bound proteins as determined by saturation transfer EPR spectroscopy. *In* Bioenergetics of Membranes. L. Packer editor. Academic Press, Inc., New York. 47–54.
45. DEBYE, P. 1945. Anomalous dispersion for radio frequencies. *In* Polar Molecules. Dover Publications, Inc., New York. 77–85.
46. TAO, T. 1968. Time-dependent fluorescence depolarization and Brownian rotational diffusion coefficients of macromolecules. *Biopolymers.* **8**:609–632.
47. BELFORD, G. G., R. L. BELFORD, and G. WEBER. 1972. Dynamics of fluorescence polarization in macromolecules. *Proc. Natl. Acad. Sci. U. S. A.* **69**:1392–1393.
48. HOLOWKA, D. A., and R. E. CATHOU. 1976. Conformation of immunoglobulin M. 2. Nanosecond fluorescence depolarization analysis of segmental flexibility in anti-ϵ-1-dimethylamino-5-naphtha lenesulfonyl-L-lysine anti-immunoglobulin from horse, pig, and shark. *Biochemistry.* **15**:3379–3390.
49. CHAN, L. M., and R. E. CATHOU. 1977. The role of the inter-heavy chain disulfide bond in modulating the flexibility of immunoglobulin G antibody. *J. Mol. Biol.* **112**:653–656.
50. MANNHERZ, H. G., J. BARRINGTON-LEIGH, K. C. HOLMES, and G. ROSENBAUM. 1971. Identification of the transitory complex myosin-ATP by the use of α,β-methylene-ATP. *Nat. New Biol.* **241**:226–229.
51. DUKE, J., R. TAKASHI, K. UE, and M. MORALES. 1976. Reciprocal reactivities of specific thiols when actin binds to myosin. *Proc. Natl. Acad. Sci. U.S.A.* **73**:302–306.
52. MCCALLEY, R. C., E. J. SHIMSHICK, and H. M. MCCONNELL. 1972. The effect of slow rotational motion on paramagnetic resonance spectra. *Chem. Phys. Lett.* **13**:115–119.
53. KÄIVÄRÄINEN, A. I., and R. S. NEZLIN. 1976. Spin-label approach to conformational properties of immunoglobulins. *Immunochemistry.* **13**:1001–1008.
54. PERRY, S. V., A. MARGRETH, and R. S. ADELSTEIN, editors. 1976. Contractile Systems in Non-Muscle Tissue. (Elsevier/North Holland, New York). 360 pp.
55. BURLEY, R. W., J. C. SEIDEL, and J. GERGELY. 1972. The stoichiometry of the reaction of the spin-labeling of F-actin and the effect of orientation of spin-labeled F-actin filaments. *Arch. Biochem. Biophys.* **146**:597–602.
56. FUJIME, S. 1970. Quasi-elastic light scattering from solutions of macromolecules. II. Doppler broadening of light scattered from solutions of semi-flexible polymers, F-actin. *J. Physiol Soc. Jpn.* **29**: 751–759.
57. FUJIME, S., and S. ISHIWATA. 1971. Dynamic characteristics of F-actin and thin filaments *in vivo* and *in vitro*. *J. Mol. Biol.* **62**:251–256.
58. OOSA WA, F., Y. MAEDA, S. FUJIME, S. ISHIWATA, T. YANAGIDA, and M. TANIGUCHI. 1977. Dynamic study of F-actin by quasielastic scattering of laser light. *J. Mechanochem. Cell Motility.* **4**:63–78.
59. TAWADA, K. 1969. Physiochemical studies of F-actin-heavy meromyosin solutions. *Biochim. Biophys. Acta.* **172**:311–318.
60. LOSCALZO, J., G. H. REED, and A. WEBER. 1975. Conformational change and cooperativity in actin filaments free of tropomyosin. *Proc. Natl. Acad. Sci. U.S.A.* **72**:3412–3415.
61. MIKI, M., T. KOUYAMA, and K. MIHASHI. 1976. Fluorescence study of ϵ-ADP bound to rabbit F-actin: structural change in the adenine subsite of F-actin under the influence of heavy meromyosin. *FEBS (Fed. Eur. Biochem. Soc.) Lett.* **66**:98–101.
62. CHERRY, R. J. 1975. Protein mobility in membranes. *FEBS (Fed. Eur. Biochem. Soc.) Lett.* **55**:1–7.
63. HIDALGO, C., N. IKEMOTO, and J. GERGELY. 1976. Role of phospholipids in the calcium-dependent ATPase of the sarcoplasmic reticulum. *J. Biol. Chem.* **251**:4224–4232.
64. TONOMURA, Y., and M. F. MORALES. 1974. Change in state of spin labels bound to sarcoplasmic reticulum with change in enzymic state, as deduced from ascorbate-quenching studies. *Proc. Natl. Acad. Sci. U.S.A.* **71**:3687–3691.
65. LINDEN, C. D., K. WRIGHT, H. M. MCCONNELL, and C. F. FOX. 1973. Lateral phase separations in

membrane lipids and the mechanism of sugar transport in *Escherichia coli*. *Proc. Natl. Acad. Sci. U.S.A.* **70**:2271–2275.

66. MARTONOSI, A., and F. FORTIER. 1974. The effect of anti-ATPase antibodies upon the Ca^{++} transport of sarcoplasmic reticulum. *Biochem. Biophys. Res. Commun.* **60**:382–389.
67. DUTTON, A., E. D. REES, and S. J. SINGER. 1976. An experiment eliminating the rotating carrier mechanism for the active transport of Ca ion in sarcoplasmic reticulum membranes. *Proc. Natl. Acad. Sci. U.S.A.* **73**:1532–1536.
68. WILKERSON, L. S., R. C. PERKINS, JR., R. ROELOFS, L. SWIFT, L. R. DALTON, and J. H. PARK. 1978. Erythrocyte membrane abnormalities in Duchenne muscular dystrophy monitored by saturation transfer EPR spectroscopy. *Proc. Natl. Acad. Sci. U.S.A.* **75**:838–841.
69. HEMMINGA, M. A., P. A. DE JAGER, and J. L. DE WIT. 1977. Saturation transfer electron paramagnetic resonance spectroscopy of spin-labeled tobacco mosaic virus protein. *Biochem. Biophys. Res. Commun.* **79**:635–639.
70. KINOSITA, K., JR., S. KAWATO, and A. IKEGAMI. 1977. A theory of fluorescence polarization decay in membranes. *Biophys. J.* **20**:289–305.